ACS ES&T Air

Open Access

pubs.acs.org/estair

Article

Influence of Relative Humidity and Seed Particles on Molecular Composition of α-Pinene Secondary Organic Aerosol

Published as part of ACS ES&T Air special issue "John H. Seinfeld Festschrift".

Jens Top, Natasha M. Garner, Félix Sari Doré, Yanjun Zhang, Cecilie Carstens, Clément Dubois, Fabian Mahrt, Markus Ammann, André S. H. Prévôt, Matthieu Riva, Imad El Haddad, and David M. Bell*

Cite This: *ACS EST Air* 2025, 2, 1565−1574

Read Online

ACCESS | Metrics & More | Article Recommendations | Supporting Information

ABSTRACT: Secondary organic aerosol (SOA), a major component of submicrometer particles, is critical to the climate and human health. SOA can form through nucleation of low-volatility organic compounds, following atmospheric oxidation, or by condensing these vapors onto existing particles. In either of these cases, the formation of SOA particles could be affected by atmospheric conditions (e.g., relative humidity (RH)) and particle liquid water content. This study examines the effects of RH on the formation and composition of SOA from dark α-pinene ($C_{10}H_{16}$) ozonolysis, as a canonical system, with or without ammonium sulfate (AS, $(NH_4)_2SO_4$) seed particles across varying RH levels. Using online extractive electrospray ionization mass spectrometry, we identified monomers (C_{7-10}) and dimers (C_{15-20}) in the SOA with high chemical and temporal resolution. In both cases, high RH (>90%) promotes dimer formation in the particle phase, while they appear at the beginning of the experiment when $(NH_4)_2SO_4$ seeds are present. The prompt increase in dimers in high RH seed containing experiments (60−65% dimers), which are absent at low RH (10%), suggests that intraparticle reactions are responsible for the dimer formation.

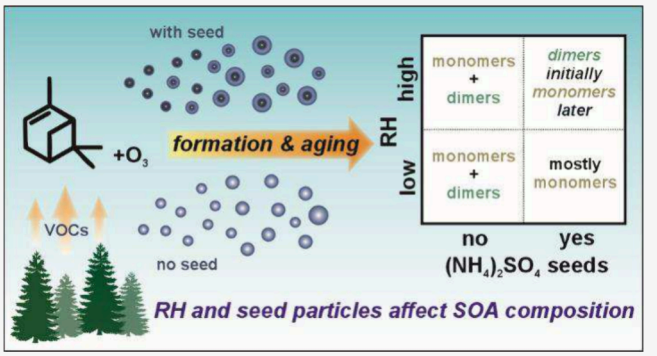

KEYWORDS: *Terpene oxidation, α-pinene, dimers, autoxidation, peroxides, SOA formation, particle phase reactions, chamber studies*

INTRODUCTION

Aerosols are harmful to human health[1,2] and impact the climate.[3] Submicron aerosols mainly consist of organic molecules and inorganic ions such as ammonium nitrate (NH_4NO_3) and ammonium sulfate ($(NH_4)_2SO_4$). Inorganic aerosols typically form through the oxidation of sulfur dioxide (SO_2) and nitrogen oxides (NO_x), resulting in sulfuric (H_2SO_4) and nitric (HNO_3) acids that can form new particles or condense onto existing aerosols. Organic aerosols may be directly emitted from incomplete combustion or generated within the atmosphere through oxidation of biogenic and anthropogenic volatile organic compounds (VOCs), forming secondary organic aerosol (SOA). SOA, which constitutes a significant portion (20−90%) of global atmospheric aerosols by mass,[4] often originates from the oxidation of biogenic VOCs (BVOCs) emitted by vegetation.

Monoterpenes ($C_{10}H_{16}$) are an important class of BVOCs, of which α-pinene is thought to have the largest contribution to SOA formation.[5] α-Pinene, specifically, represents a major source of SOA even in isoprene rich areas.[6,7] α-Pinene is rapidly oxidized by ozone (O_3), hydroxy radicals (OH), or nitrate radicals (NO_3) to form peroxy radicals (RO_2). RO_2 radicals can undergo autoxidation, which involves sequential intramolecular hydrogen transfers and molecular oxygen additions, resulting in highly oxygenated radicals.[8,9] The process ends with bimolecular reactions that generate oxygenated organic molecules (OOMs), including monomers or covalently bound low, extra-low, and ultralow volatility dimers (ROOR′).[10] Autoxidation and dimerization are key for new particle formation, and their importance for SOA mass needs to be determined.

Beyond gas-phase formation, prior research has observed that OOMs and dimers also evolve in the particle phase. For example, using extractive electrospray ionization time-of-flight mass spectrometry (EESI-TOF), Pospisilova et al.[11] demon-

Received: March 2, 2025
Revised: May 29, 2025
Accepted: May 30, 2025
Published: July 7, 2025

strated that condensed-phase reactions rapidly alter the composition of OOMs. Kenseth et al.[12] further confirmed particle-phase dimer formation using synthesized standards. However, the relative contributions of gas-phase versus particle-phase processes to the formation of the OOMs and dimers remain unclear.

Furthermore, biogenic SOA frequently interacts with preexisting particles, mixing with inorganic aerosols, which can influence SOA composition and physical properties.[13,14] Inorganic salts that are often present in seed particles, such as sulfate (SO_4^{2-}) and nitrate (NO_3^-), contribute to the particle composition in several ways. First, they increase liquid water content due to their higher hygroscopic growth factors (>1.5 at 84% relative humidity (RH))[15] compared to SOA (~1.1 at 84% RH).[15] Second, inorganics may react with condensed-phase organics to form, e.g., organosulfates.[16−18] Additionally, inorganics affect aerosol pH, which can promote dimer formation and other reactions under acidic conditions.[19,20] In laboratory settings, inorganic seed particles increase available surface area, competing with chamber walls for condensable vapors.[21,22]

Surdu et al.[23] recently showed that water taken up into the particles at elevated RH acts as a plasticizer, reducing viscosity and increasing molecular diffusivity in the particle phase, thereby promoting SOA formation. These findings underscore the importance of understanding how both inorganic seeds and water impact SOA composition and reactivity. Despite the prevalence of water in the troposphere and its significant role in SOA formation, only very few chamber experiments have been conducted at high humidity (>75% RH).[24] Some studies include the work by Qin et al.[25] who reported no dependence of chemical composition of α-pinene SOA on RH. Their study employed an aerosol mass spectrometer (AMS) used for the chemical speciation of the particle phase, a technique based on a hard ionization method. As a result, molecular formulas could not be directly determined. Instead, particles were classified into broad categories (C_xH_y, C_xH_yO, and $C_xH_yO_z$) which, together with O:C and H:C ratios, were used to infer compositional changes. While informative, this approach limited detailed insights into chemical processes. Zhang et al.[26] reported a series of experiments where unsubstituted and deuterated α-pinene were oxidized at 40% RH using an oxidation flow reactor. While this study provided valuable insight into intramolecular hydrogen shift as a driver of OOM formation, no comparison between different humidities was made. Zhang et al.[27] carried out α-pinene ozonolysis in a chamber, sampled the SOA using a PILS system and, using LCMS, reported temporal profiles of SOA components. They showed a slight increase in SOA yield with rising RH, and they further identified prompt formation of SOA dimers, which they attributed to particle phase reactions. Though none of these studies included inorganic seed particles, which can significantly modulate aerosol liquid water content. Recently, Luo at al.[28] compared the absence and presence of ammonium sulfate (AS, $(NH_4)_2SO_4$) seed particles and the relative humidity on the α-pinene ozonolysis system in a series of flow tube experiments utilizing EESI-TOF, allowing for chemical speciation. They found that, in the presence of AS seeds, RH has no significant impact on SOA chemical composition, while in the absence of AS seeds, increasing RH leads to a larger fraction of monomers (C_{4-10}) versus dimers (C_{16-20}). However, their analysis is limited to the first 15 min after the VOC injection. While these studies provide some insight into the complex interplay between RH, inorganic seed particles, and α-pinene ozonolysis, their detailed investigation is still lacking. Therefore, further studies are required to elucidate these effects, since they can have profound impacts on SOA composition, as we will demonstrate here.

In this study, we investigate the interplay among RH, inorganic seed, and SOA chemical composition. The evolution of the chemical composition of SOA under different conditions (RH and inorganic seeds) provides insight into the impact of intraparticle reactions during the formation and aging of α-pinene SOA. An electrospray ionization time-of-flight mass spectrometer (EESI-ToF)[29,30] was used for the high temporal and molecular-level identification of condensed phase oxidation products, including monomers (C_{7-10}) and dimers (C_{15-20}). We show that both RH and seed particles affect the ratio of monomers to dimers formed. Increased RH generally promotes dimer formation, whereas ammonium sulfate seed particles compete with the walls for condensable organic vapors and influence condensed-phase reaction time scales, promoting faster appearance of dimers in the particle phase. Furthermore, we explore these differences to hypothesize about the formation pathway of the dimers (e.g., gas phase vs condensed phase).

MATERIALS AND METHODS

SOA Formation and Aging Experiments. Experiments were carried out in an ~9 m^3 atmospheric simulation chamber, consisting of a fluorinated ethylene propylene bag housed in an enclosure that was temperature-controlled to 18 ± 0.5 °C for all experiments described herein.[31,32] Prior to each experiment, the chamber was flushed with dry, VOC, and NO_x free air at 50 L min^{-1} from a zero-air generator (737−250 series; AADCO Instruments, Inc., USA). This resulted in aerosol number concentrations below 10 particles cm^{-3}, as verified using a scanning mobility particle sizer (SMPS, consisting of a model 3081 differential mobility analyzer and a model 3775 condensation particle counter; TSI, Inc., USA). The chamber was then filled with either dry or humidified air to achieve either low or high RH conditions. Humidified air was generated by passing 20−30 L min^{-1} zero air through a 2 L round-bottom flask containing 18.2 MΩ·cm Milli-Q water (MilliporeSigma, Germany), while chamber RH was monitored using a humidity sensor (HMP 110, Vaisala, Finland). For low RH experiments, the chamber was kept below 10% RH. For high RH experiments, the chamber was set between 90% and 95% RH, which ensured that the aerosol remained deliquesced throughout the experiment.

At both low RH and high RH conditions, experiments were performed where SOA was formed and aged in both the presence and absence of AS seed particles. A detailed description of the seed experiments can be found in Garner et al.[33] Briefly, at the beginning of the seed experiments, polydisperse seed particles were directly nebulized into the chamber from an aqueous solution containing 1 ppm of AS (Sigma-Aldrich, purity > 99.5%) in 18.2 MΩ cm Milli-Q water, using a home-built nebulizer. Seed particles were added until a dry mass concentration of ~130 $\mu g\ m^{-3}$ was reached, as continuously measured by SMPS, assuming a density of 1.77 g cm^{-3}. For further analysis of the SOA, a density of 1.2 g cm^{-3} was used.[34] O_3 was generated and added to the chamber by passing dry air through a UV lamp (UVC, 254 nm) and continuously measured by an O_3 monitor (TEI 49C, Thermo Environmental Instruments, USA). For the nonseeded experi-

https://doi.org/10.1021/acsestair.5c00064
ACS EST Air 2025, 2, 1565−1574

ments, this step occurred immediately after the desired RH was reached in the chamber. Using a syringe, 3.2 μL of α-pinene (TCI, purity >97.0%), corresponding to a mixing ratio of ~50 ppb, was then injected through a heated septum (80 °C), where it evaporated immediately and was flushed (60 L min^{-1}) into the chamber by clean air from the zero-air generator. The mixing ratio of O_3 and α-pinene was kept constant for both seeded and nonseeded experiments. The experimental conditions chosen avoided new particle formation during the seeded experiments.

No OH scavenger was used in the experiments presented in this work, since adding an OH scavenger does not decouple the OH and O_3 chemistry in a straightforward way.[35] Figure S4 in the Supporting Information shows a modeled comparison of the reactivity of both OH and O_3 toward α-pinene, showing that O_3 accounts for ~80% of the α-pinene reactivity, making us confident that the results reported are representative for α-pinene ozonolysis.

Aerosol Measurements. Throughout the experiments, the particle number size distribution was continuously monitored using a SMPS. The SMPS was equipped with a Nafion dryer upstream of its inlet, such that the reported aerosol mass corresponds to dried particles. The SOA chemical composition was measured with an online extractive electrospray ionization time-of-flight mass spectrometer (EESI-ToF; Tofwerk, Switzerland).[29,30] The EESI-TOF consists of a home-built EESI inlet[29] coupled to an atmospheric pressure interface time-of-flight mass spectrometer (API-TOF; Tofwerk, Switzerland), which has a resolution of ~5000 ΔM/M. Aerosol was continuously sampled from the chamber at a flow rate of ~0.8 L min^{-1}. The flow was sampled into a plume of charged droplets, generated by the electrospray probe from a 100 ppm solution of NaI in 18.2 MΩ cm of Milli-Q water. Positive ion mass spectra were recorded at 1 Hz, and all ions were detected as adducts with Na^+. Spray stability was ensured by observing the reagent ion Na_2I^+ at 172.88 m/z prior to α-pinene injection. The electrospray was operated at 2850 or 2900 V, and the voltage was kept constant throughout the entire experiment.

Analysis of EESI-ToF data were performed using Tofware version 3.2.5 (Tofwerk, Switzerland). 1 Hz data were averaged to 10 s before high-resolution peak fitting was performed for the m/z range of 95 to 535. Fitted peaks were assigned to molecular formulas with carbon number ranging from C_2 to C_{20}. The 5 min sample intervals were alternated with 90 s background intervals by sampling chamber air through a high efficiency particulate air (HEPA) filter to remove particles. For both sample and background measurements, the airflow went through a multichannel extruded carbon denuder (6 mm inner diameter 5 cm long), which was baked every 2 weeks at 200 °C while passing N_2 through it. The denuder removed gaseous species and ensured an ~10 s response when shifting from the sample to the background and back to the sample. Reported signals were determined as the difference between the sample and the average background signal immediately before and after each measurement period. Data were then averaged over the 6.5 min total sampling time (sample plus background), resulting in one data point per sample interval. Additionally, data were normalized to the primary ion, which was Na_2I^+ in all our experiments. EESI-ToF signals are reported as a mass flux of ions (in attogram per second; ag s^{-1}) reaching the mass spectrometer microchannel detector. To determine the ion mass flux, φ_m, the measured EESI-ToF signal was converted as follows:

$$\varphi_m = \frac{\mathrm{EESI(Hz)} \cdot M \cdot 10^{18}}{N_a} \quad (1)$$

where M is the molar weight of the ion and N_a is Avogadro's number ($6.022 \cdot 10^{23}$ mol^{-1}).

Modeling the Depletion of Gas Phase α-Pinene. The depletion of gas-phase α-pinene was simulated using the F0AM 0D atmospheric box model.[36] The model was run using a subset of the Master Chemical Mechanism (MCM, version 3.3.1),[37,38] which included 314 species and 942 reactions pertinent to the α-pinene reactions. Initial conditions were set to 50 ppb α-pinene and 300 ppb of O_3, and model simulations were run at both low (5%) and high (95%) RH to simulate the depletion of α-pinene under the different experimental conditions covered in this work.

RESULTS AND DISCUSSION

SOA Formation. Figure 1 shows the time series of the average aerosol mass generated by dark ozonolysis of α-pinene

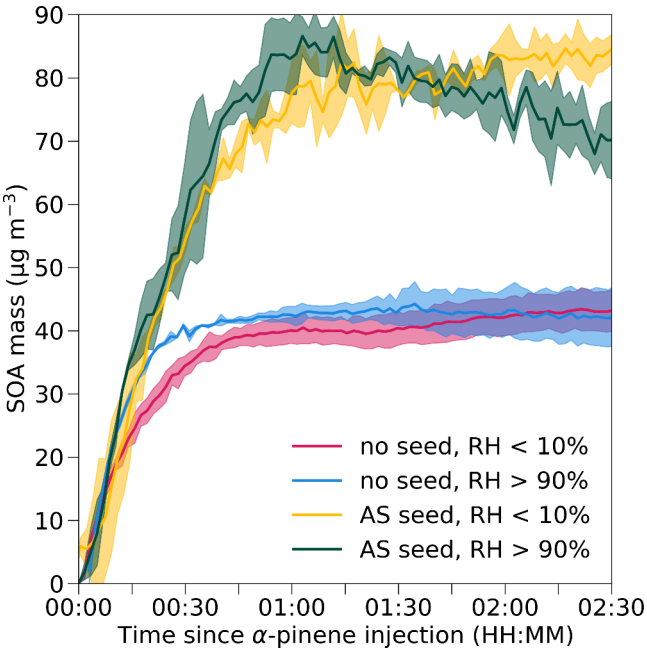

Figure 1. Time series of average organic aerosol mass (μg m^{-3}) generated by dark ozonolysis of α-pinene at low and high RH in the absence and presence of polydisperse ammonium sulfate seed particles, as measured by SMPS. Uncertainties (±1 standard deviation) are indicated by shaded regions.

at low and high RH, in both the absence and presence of AS seed particles. The reported SOA mass for the experiments in the presence of AS seeds only includes the organic mass fraction. It was determined by subtracting the inorganic seed mass measured at the time of α-pinene injection from the total particle mass as measured by SMPS. All experiments are corrected for particle-phase wall losses, as described in the Supporting Information (SI) Section S1.

In the absence of AS seeds, a 40 μg m^{-3} SOA mass rapidly formed within 30 min of α-pinene injection under both low and high RH conditions. For the remainder of the experiment, the particulate mass remained effectively constant. In contrast,

https://doi.org/10.1021/acsestair.5c00064
ACS EST Air 2025, 2, 1565−1574

in the presence of AS seeds, a maximum of ~80 μg m^{-3} was formed at both low and high RH values within the first ~60 min. In Table S2, we show the SOA yields for each experimental condition. This illustrates that substantially more SOA mass was formed in the presence of the AS seeds. The enhanced SOA formation in the presence of seeds is expected, given that seed particles provide a surface for the gas-phase oxidation products to partition to, competing with loss of vapors to the chamber walls.[22] In seeded experiments under high RH, the mass drops, indicating the potential consumption of oxidation products with subsequent evaporation.

Chemical Composition of SOA Formed in the Absence and Presence of AS Seed Particles. Figure 2 shows a correlation matrix of EESI-ToF mass spectra recorded after 1 h of SOA formation, corresponding to the moment at which the maximum mass was reached in the seeded experiments. Details about its construction are given in Section S2 in the Supporting Information. The matrix highlights strong, positive correlations with R > 0.9 between repeat experiments under identical conditions, demonstrating high experimental reproducibility. In contrast, experiments under different conditions show more variability, particularly between low and high RH, where R drops to 0.7, highlighting that RH modulates the SOA molecular composition.

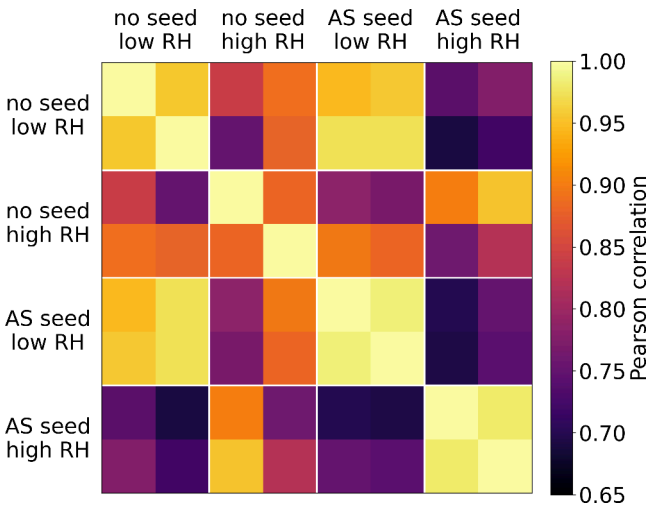

Figure 2. Correlation matrix showing the Pearson correlation coefficient between average mass spectra measured by the EESI-ToF, calculated for all independent experiments (small squares) that were performed under a given experimental condition. The different experimental conditions investigated are indicated on the left and top axes and include experiments without and with ammonium sulfate (AS) seeds and low and high relative humidity (RH) conditions, respectively.

Figure 3 summarizes the chemical composition of the SOA mass spectra along with the key monomer ($C_{7-10}H_xO_y$) and dimer ($C_{15-20}H_xO_y$) species. Under all conditions, the dominant compounds were $C_9H_{14}O_{4-6}$ and $C_{10}H_{16}O_{4-6}$ monomers The appearance of $C_{10}H_{16}O_{4-6}$ is expected since α-pinene's molecular formula is $C_{10}H_{16}$, while $C_9H_{14}O_{4-6}$ molecules were previously reported.[27,28] Nevertheless, in low RH experiments, $C_{10}H_{16}O_x$ molecules were the most abundant carbon series, whereas in high RH experiments, $C_9H_{14}O_x$ molecules dominated. This was independent of the presence or absence of seed particles, indicating that this shift in composition toward $C_9H_{14}O_x$ is driven by differences in aerosol water content.

Without accounting for sensitivity differences between monomers and dimers (likely underestimated here)[39] under low RH conditions and in the absence of seed particles (Figure 3A), in terms of mass weighted signal (ag s^{-1}), approximately 60% of condensed-phase organic species are monomers and 40% are dimers. Among the dimers, contributions from C_{17}, C_{18}, C_{19}, and C_{20} were nearly equal (~10%, respectively). In comparison, in the presence of seed particles (Figure 3B), about 71% of the organic species detected were monomers (31% C_{7-9} and 40% C_{10}), with a notable increase in C_{10} species at the expense of C_{15-18} compounds. This shift from dimers to monomers may be attributed to enhanced partitioning, as the increased aerosol surface area facilitates the condensation of more volatile species. Figure S5 in the Supporting Information illustrates the increase in surface area due to increasing RH. As shown in Figure 1, the presence of seed particles generates approximately 50% more particle mass, explaining part of the shift in the monomer-to-dimer ratio (i.e., $\Sigma C_{7-10}H_xO_y/\Sigma C_{15-20}H_xO_y$).

Figure S2 further compares these two scenarios at earlier stages (15 and 30 min) of particle formation, when wall loss effects are greatest for low-volatility species. In the absence of seed particles, the monomer-to-dimer ratio remains relatively stable. However, with seeds present, the monomer fraction rises significantly, from 52% at 15 min to 71% at 60 min, coinciding with an increase in aerosol mass from ~30 to 75 μg m^{-3} (Figure 1). This shift reflects further partitioning of volatile-gas-phase monomers as particle mass increases. In the absence of seeds, these monomers are likely lost to the chamber walls, reducing the availability for particle growth and resulting in the observed lower monomer-to-dimer ratio.

Comparing the low RH no-seed condition (Figure 3A) to the high RH no-seed condition (Figure 3C), we observed a shift toward more monomers, primarily driven by an increase in C_{7-9} monomers, particularly $C_9H_{14}O_4$ and $C_9H_{14}O_5$. There is also a noticeable shift toward less oxygenated species, with a marked reduction in O_{7+} species, consistent with the findings of Surdu et al.[23] Figure 3D shows the high RH condition with seed particles. The trend toward a (relative) increase in C_9 molecules remains consistent with that observed for the high RH no-seed case (Figure 3C). Additionally, a significant increase in dimers is observed, now constituting approximately 49% of the total signal.

The compositional changes going from low to high RH conditions observed for both seeded and unseeded experiments cannot be attributed solely to a reduced dynamic viscosity of the SOA material and enhanced gas-to-particle partitioning. Unlike the findings of Surdu et al.,[23] where only low-oxygen components increased in the particle phase, here, we observed a clear shift from C_{10}- to C_9-dominated composition with added water. This suggests that particle-phase reactions involving fragmentation and dimer formation are occurring within the aerosol. Of course dimer decomposition could also result in formation of these species at high RH, but the general increase in dimers when seeds are present and the constant fraction of dimers when going from low to high RH when no seeds are present suggest that if this is an important pathway it must be equally compensated by another dimer formation pathway. Decomposition and loss of highly oxygenated molecules (HOMs) could be a source of OH radicals, which would contribute to the observed fragmentation

https://doi.org/10.1021/acsestair.5c00064
ACS EST Air 2025, 2, 1565−1574

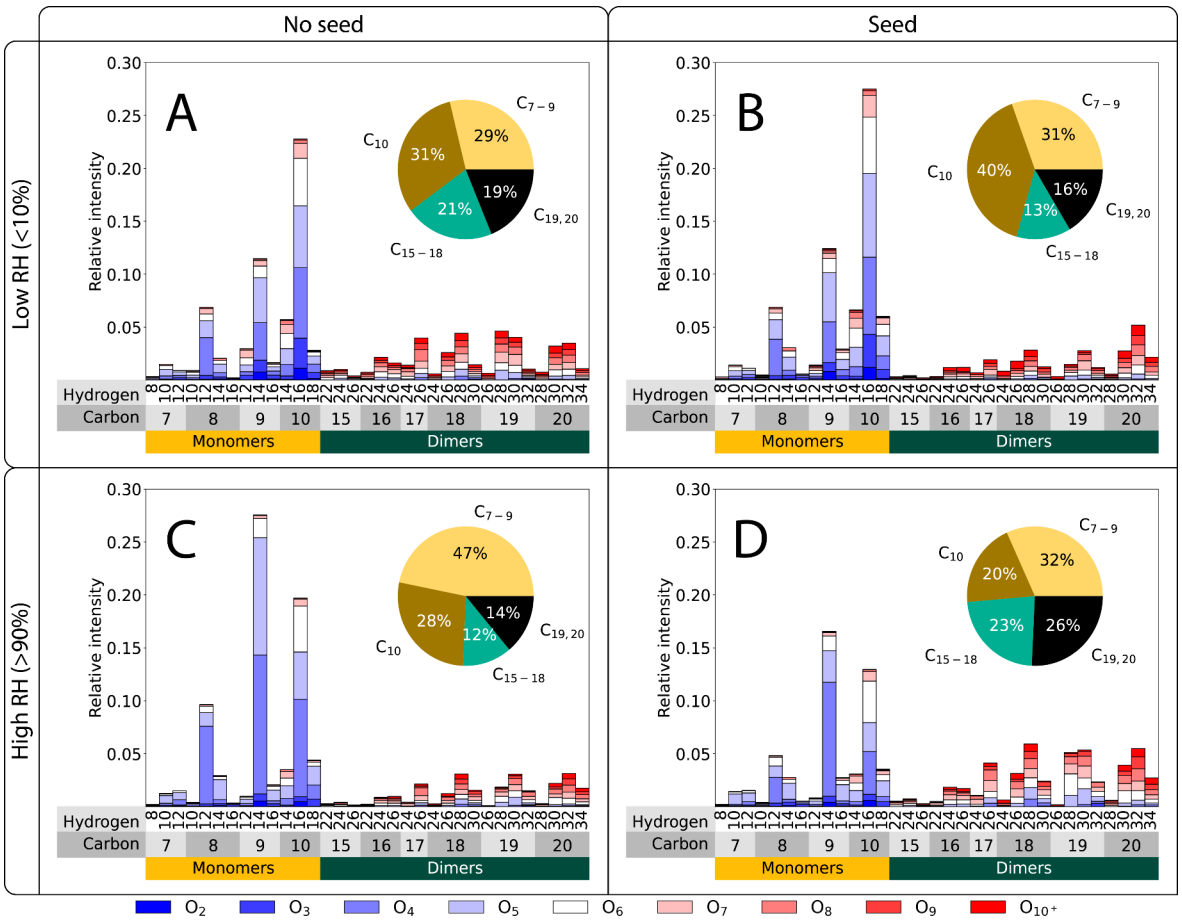

Figure 3. Bar graphs of key monomers and dimers 1 h after the start of SOA formation under the different experimental conditions: (A) low RH, no AS seed particles; (B) low RH, AS seed particles; (C) high RH, no seed particles; (D) high RH, AS seed particles. The pie charts show the relative contributions of the representative monomers and dimers.

(e.g., C_{10} to C_8 and C_9) and possibly enhanced dimer formation.

Temporal Evolution of Monomer and Dimer Composition. In the next section, the time series showing the gas phase consumption of α-pinene will be compared against the time series of the different aerosol components to provide insight into what drives the formation of various monomer and dimer species. At present, because the relative importance of condensed phase reactions cannot be quantified, we decided to forego a discussion about the mechanistic impacts. Since we only obtain molecular formula information from our EESI-MS data, we are unable to elucidate the exact reaction pathways that others have been able to show (e.g., Kenseth et al.[12]); this would require information on the functionality and structure of our condensed phase species. This makes us reluctant to over interpret our results in this paper. Additionally, this level of analysis is not unlike other recent literature for aerosol phase reactions, e.g., Zhao et al.[40] We are currently working on using thermal desorption (TD) EESI to study monomers and dimers more quantitatively[39] and plan to study these reaction pathways in more detail in the future.

In Figure 4, we show the relative monomer (C_{7-9} and C_{10}) and dimer (C_{15-18} and C_{19-20}) time series for selected experiments. Additionally, we show the corresponding time series on an absolute scale in Figure 5, in addition to the consumption of α-pinene in the gas phase modeled by F0AM.

For the two low-RH conditions (Figure 5A,B), monomer trends generally follow the consumption of α-pinene, while the dimer region shows notable differences. In the no-seed experiment, there is a steady increase in the C_{15-18} fraction (light green), which is absent in the seeded experiment. Figure 4A,B highlights the overall higher monomer fraction in the seeded experiment, likely due to increased monomer partitioning as discussed above. In the no-seed low RH experiment, the absolute dimer signal steadily increases (Figure 5A), but the dimer fraction only rises slightly from 40% to 45% (Figure 4A), driven exclusively by the C_{15-18} compounds. This suggests that continued dimer formation involves particle-phase reactions, where C_{17-18} likely forms from C_{10} + C_{8-7} or C_9 + C_{8-9} precursors, while C_{15-16} forms from fragmentation of C_{17-18} compounds.

Figures 4C and 5C show the time series for high RH conditions without seed particles present, and the temporal evolution of both monomer classes depicted follows the depletion of α-pinene vapors. In contrast, the formation of dimers (both C_{15-18} and $C_{19,20}$) initially proceeds more slowly than the depletion of gas phase α-pinene. However, at longer aging times, the dimer formation is observed to continue after the plateau of the monomers. In Figure 4C, the fraction of dimers slowly increases from 40% to 50% at the end of the experiment. Since steady formation well after the consumption of α-pinene is observed, processes other than gas-phase

https://doi.org/10.1021/acsestair.5c00064
ACS EST Air 2025, 2, 1565−1574

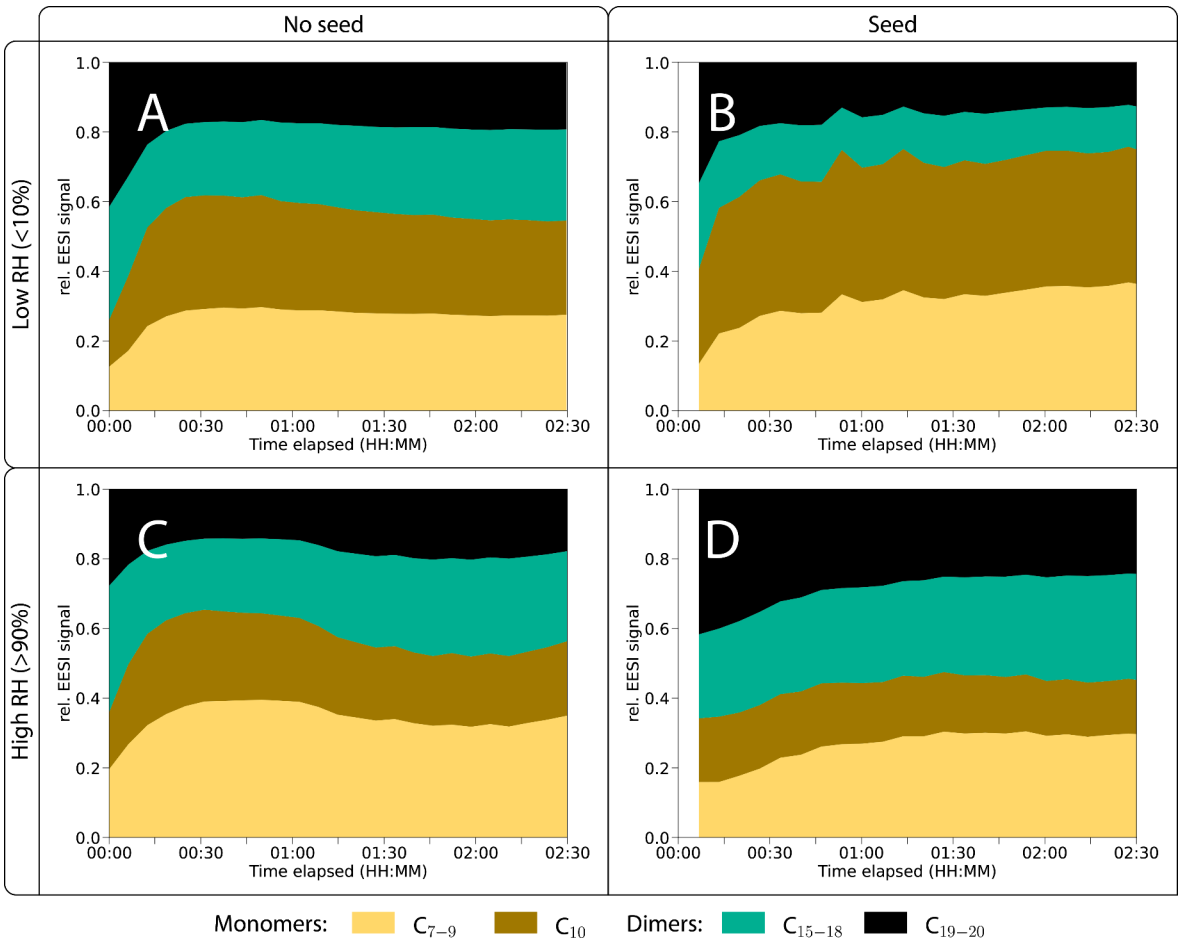

Figure 4. Monomer (brown shades) and dimer (green shades) fraction time series under the different experimental conditions: (A) low RH, no seed particles; (B) low RH, AS seed particles; (C) high RH, no seed particles; (D) high RH, AS seed particles. Time 00:00 corresponds to α-pinene injection.

reactions, i.e., formation due to intraparticle reactions (e.g., fragmentation or dimer formation), must be responsible.

Figures 4D and 5D show the time series for the high RH seeded experimental conditions, reiterating the initially much larger prevalence of dimers already seen, which in Figure 3D showed a much larger prevalence of dimers. The monomer evolution is qualitatively similar to the time series shown in Figure 5C (high RH, no seeds) and in agreement with Figure 3C,D. However, Figures 4 and 5D show that the C_{19-20} dimers are promptly observed upon oxidation and then decay throughout the experiment. The strong initial dimer formation is not observed in the dry seed case, suggesting that a fraction of these dimers is likely formed promptly in the particle phase. The prompt decay of C_{19-20} dimers in comparison to all other experiments suggests that seed particles (and potentially their high liquid water content) facilitate the reactions of these dimers. The C_{15-18} dimers increase steadily at a rate similar to that of the gas phase α-pinene consumption, though the correlation between C_{15-18} dimers and the α-pinene consumption could be misleading, as the (promptly) formed C_{19-20} dimers could fragment to form C_{15-18} products. Overall, the dimers begin by making up 70% of the SOA composition in 15 min, which changes to 40% in 2 h (Figure 4D). The decrease in the dimer fraction coincides with the increase in the concentration of C_9 compounds, probably resulting from fragmentation.

The difference in the dynamics of the dimers between the two seed experiments indicates that the presence of water plays a significant role in the formation and evolution of dimers. This should be reflected in changes in the volatility distribution, meaning that at high RH (with a large fraction of dimers) the volatility of the SOA should be substantially lower than under low RH conditions (dominated by monomers). Similarly, aging will also decrease the volatility of the particle-phase compounds through steady reactions taking place within the aerosol phase, but this is expected only to occur to a significant degree within SOA at high RH. This hypothesis was confirmed in volatility measurements of α-pinene SOA (without seeds) fresh and after 1 day of aging.[41] In these experiments, the volume fraction remaining after 24 h of evaporation, which comes from nonvolatile material (e.g., dimers and higher order oligomers), increased more when aged at 90% RH (from ~18% to 60%) in comparison to the limited changes observed within the α-pinene SOA aged at 0% RH (from ~30% to 40%). Overall, this indicates that the liquid water content plays an important role in the formation of dimers (or oligomers) and their dynamics within the aerosol phase.

Luo et al.[28] employed EESI-ToF to study α-pinene SOA formed under low and high RH and in both the presence and absence of AS seed particles, analogous to our present study. Unlike our study, they found no strong dependence on RH for SOA formed in the presence of AS seed particles. It should be

https://doi.org/10.1021/acsestair.5c00064
ACS EST Air 2025, 2, 1565−1574

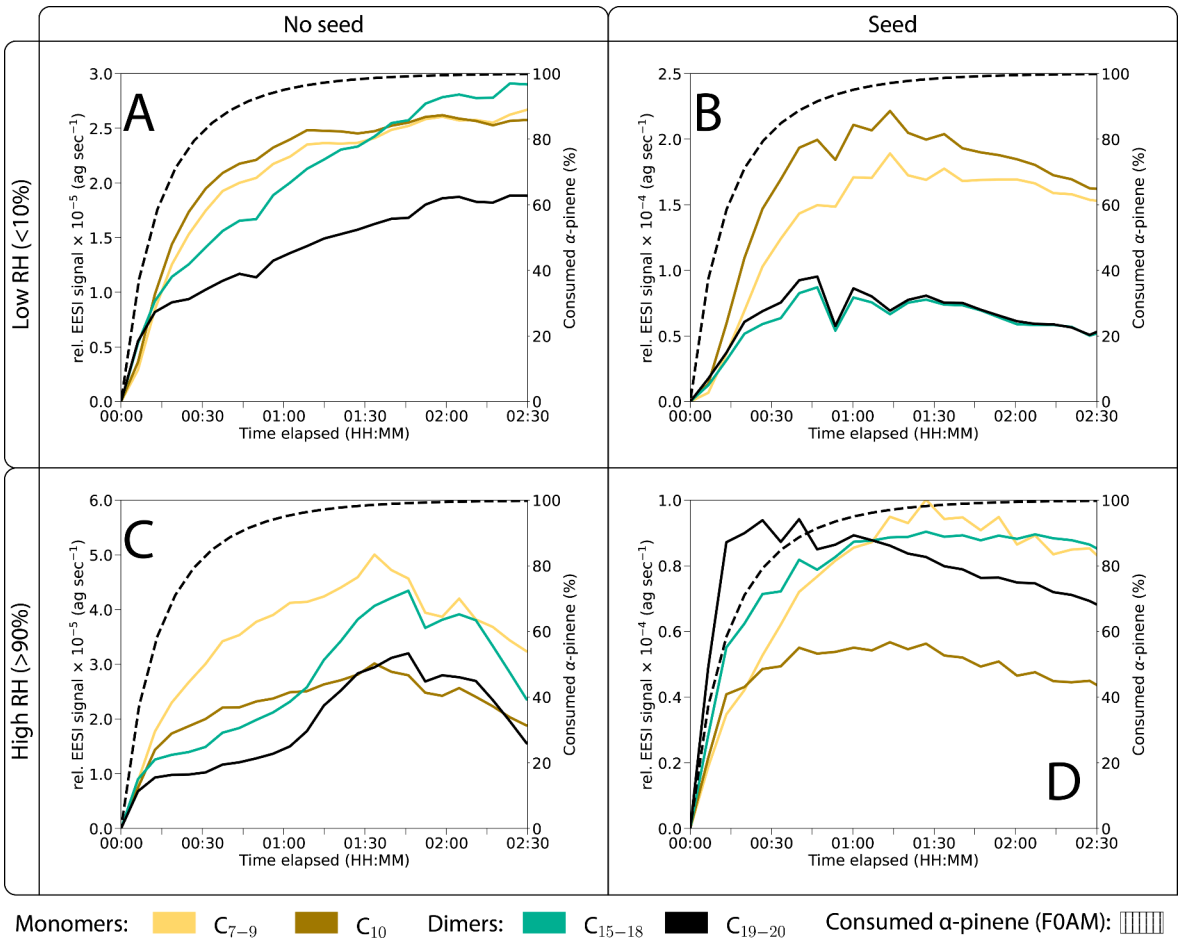

Figure 5. Particle phase time series for monomers (brown shades) and dimers (green shades) for selected experiments under the different experimental conditions: (A) low RH, no seed particles; (B) low RH, AS seed particles; (C) high RH, no seed particles; (D) high RH, AS seed particles. Time 00:00 corresponds to α-pinene injection. The consumption of gas phase α-pinene, as modeled by F0AM 0D, is shown as a dotted line.

noted, however, that they carried out their experiments in a flow tube with a residence time of 15 min and that they report EESI results for only the first 15 min after VOC injection. As is evident from Figures 4 and 5B,D, the first 15 min after VOC injection exhibit considerable variability. Moreover, it takes about 1 h for the changes in the monomers and dimers to become apparent. These results further underline the need for online instruments with both high temporal and chemical resolution when studying the α-pinene ozonolysis system such as the EESI-TOF used in the present study.

Atmospheric Implications. Overall, our results demonstrate that both the presence of water and AS seed particles can considerably influence the composition and evolution of α-pinene SOA on a molecular level. Although exact changes in molecular structure and functionality cannot be determined here, we demonstrate that there are indeed changes to the molecular formula of the species observed within α-pinene SOA, indicating that condensed-phase chemistry takes place. Specifically, the formation and evolution of large molecular weight dimers (C_{15-20}) are particularly sensitive to the presence of water and seeds, with high RH conditions promoting their formation either during the initial formation (in the presence of seeds) or steadily over time (without seeds). The dynamics of dimer formation are particularly of interest because they represent species that will not readily undergo partitioning from the particle phase back to the gas phase. Thus, dimer species are more likely to undergo long-range transport within aerosols. Furthermore, they can act as an organic phase to promote partitioning of semivolatile organics and contribute to the total particulate aerosol mass, with implications for air quality and climate.

In addition to changes in the chemical composition of particles, the dynamics associated with dimer formation likely impact microphysical aerosol properties, e.g., viscosity and phase state.[42] As such, the stark differences in SOA composition observed here warrant further investigations into the role of both water content and inorganic seed composition to determine if these specific observations are consistent across many different types of SOA or if they are specifically of interest in α-pinene SOA.

This study provides critical insight into SOA formation in the atmosphere by purely changing 2 common parameters (humidity and inorganic seed particles). The stark differences in the chemical composition of SOA observed here underscore the need to better understand the dynamics of SOA composition with relevant atmospheric water content and pre-existing seed particles. Moving toward more quantitative results would afford a better picture of the importance of aerosol condensed (or particle) phase reactions. Though as a first step, reducing uncertainties in SOA formation and

https://doi.org/10.1021/acsestair.5c00064
ACS EST Air 2025, 2, 1565−1574

evolution requires an understanding of the processes occurring when forming on pre-existing particles under a variety of humidities, which extends beyond the range of conditions explored in most atmospheric simulation chamber experiments to date.[24]

■ ASSOCIATED CONTENT

Supporting Information

The Supporting Information is available free of charge at https://pubs.acs.org/doi/10.1021/acsestair.5c00064.

Summary of experiments conducted (Table S1), mass spectra of key monomers and dimers at 1 h (Figure S1), bar graphs of key monomers and dimers under dry conditions at 15 min, 30 min, and 1 h (Figure S2), and EESI-TOF time series without wall loss correction (Figure S3) (PDF)

■ AUTHOR INFORMATION

Corresponding Author

David M. Bell − *PSI Center for Energy and Environmental Sciences, 5232 Villigen PSI, Switzerland;* orcid.org/0000-0002-3958-2138; Email: david.bell@psi.ch

Authors

Jens Top − *PSI Center for Energy and Environmental Sciences, 5232 Villigen PSI, Switzerland;* orcid.org/0000-0003-3318-4451

Natasha M. Garner − *PSI Center for Energy and Environmental Sciences, 5232 Villigen PSI, Switzerland;* orcid.org/0009-0001-0710-1432

Félix Sari Doré − *Université Claude Bernard Lyon 1, CNRS, IRCELYON, Villeurbanne F-69100, France;* Present Address: Department of Chemistry and Molecular Biology, Atmospheric Science, University of Gothenburg, SE-41390 Gothenburg, Sweden

Yanjun Zhang − *Université Claude Bernard Lyon 1, CNRS, IRCELYON, Villeurbanne F-69100, France*

Cecilie Carstens − *Université Claude Bernard Lyon 1, CNRS, IRCELYON, Villeurbanne F-69100, France*

Clément Dubois − *Université Claude Bernard Lyon 1, CNRS, IRCELYON, Villeurbanne F-69100, France;* Present Address: Department of Chemistry, Aarhus University, 8000 Aarhus, Denmark

Fabian Mahrt − *PSI Center for Energy and Environmental Sciences, 5232 Villigen PSI, Switzerland;* Present Address: Department of Chemistry, Aarhus University, 8000 Aarhus, Denmark; orcid.org/0000-0002-7059-6765

Markus Ammann − *PSI Center for Energy and Environmental Sciences, 5232 Villigen PSI, Switzerland;* orcid.org/0000-0001-5922-9000

André S. H. Prévôt − *PSI Center for Energy and Environmental Sciences, 5232 Villigen PSI, Switzerland;* orcid.org/0000-0002-9243-8194

Matthieu Riva − *Université Claude Bernard Lyon 1, CNRS, IRCELYON, Villeurbanne F-69100, France;* orcid.org/0000-0003-0054-4131

Imad El Haddad − *PSI Center for Energy and Environmental Sciences, 5232 Villigen PSI, Switzerland; College of Environmental Sciences and Engineering, Peking University, 100084 Beijing, China;* orcid.org/0000-0002-2461-7238

Complete contact information is available at: https://pubs.acs.org/10.1021/acsestair.5c00064

Author Contributions

D.M.B., I.E.H., M.A., A.S.H.P, and M.R. conceptualized the experiments. J.T., N.M.G., F.M., F.S.D., Y.Z., C.C., C.D., and D.M.B. conducted the experiments. J.T. and N.M.G. analyzed the data. J.T. wrote the manuscript with assistance from N.M.G., F.M., and D.M.B. All authors provided feedback on the manuscript and have given approval to the final version.

Funding

This work was supported by the Swiss National Science Foundation (grant nos. 188662, 200021_213071, and 206021_198140) and by the European Research Council Grant (ERC-StG MAARvEL; 423 No. 852161). N.M.G. and F.M. acknowledge funding from the European Union's Horizon 2020 research and innovation program under the Marie Skłodowska-Curie grant agreement (grant no. 884104 and grant no. 890200, respectively). Funding was also provided under the ATMO-ACCESS Integrating Activity under grant agreement no. 101008004. PSI's atmospheric simulation chamber is a facility of the ACTRIS ERIC and receives funding from the Swiss State Secretariat for Education, Research and Innovation (SERI).

Notes

The authors declare no competing financial interest.

■ REFERENCES

(1) Pope, C. A., III; Dockery, D. W. Health Effects of Fine Particulate Air Pollution: Lines that Connect. *J. Air Waste Manage. Assoc.* **2006**, *56* (6), 709−742.

(2) Burnett, R.; Chen, H.; Szyszkowicz, M.; Fann, N.; Hubbell, B.; Pope, C. A., III; Apte, J. S.; Brauer, M.; Cohen, A.; Weichenthal, S.; et al. Global estimates of mortality associated with long-term exposure to outdoor fine particulate matter. *Proc. Natl. Acad. Sci. U. S. A.* **2018**, *115* (38), 9592−9597.

(3) Intergovernmental Panel on Climate Change The Earth's Energy Budget, Climate Feedbacks and Climate Sensitivity. In *Climate Change 2021−The Physical Science Basis: Working Group I Contribution to the Sixth Assessment Report of the Intergovernmental Panel on Climate Change*; Cambridge University Press, 2023; pp 923−1054.

(4) Jimenez, J. L.; Canagaratna, M. R.; Donahue, N. M.; Prévôt, A. S. H.; Zhang, Q.; Kroll, J. H.; DeCarlo, P. F.; Allan, J. D.; Coe, H.; Ng, N. L.; et al. Evolution of Organic Aerosols in the Atmosphere. *Science* **2009**, *326* (5959), 1525−1529.

(5) Guenther, A. B.; Jiang, X.; Heald, C. L.; Sakulyanontvittaya, T.; Duhl, T.; Emmons, L. K.; Wang, X. The Model of Emissions of Gases and Aerosols from Nature version 2.1 (MEGAN2.1): an extended and updated framework for modeling biogenic emissions. *Geoscientific Model Development* **2012**, *5* (6), 1471−1492.

(6) Ayres, B. R.; Allen, H. M.; Draper, D. C.; Brown, S. S.; Wild, R. J.; Jimenez, J. L.; Day, D. A.; Campuzano-Jost, P.; Hu, W.; de Gouw, J.; et al. Organic nitrate aerosol formation via NO_3 + biogenic volatile organic compounds in the southeastern United States. *Atmospheric Chemistry and Physics* **2015**, *15* (23), 13377−13392.

(7) Sareen, N.; Carlton, A. G.; Surratt, J. D.; Gold, A.; Lee, B.; Lopez-Hilfiker, F. D.; Mohr, C.; Thornton, J. A.; Zhang, Z.; Lim, Y. B.; et al. Identifying precursors and aqueous organic aerosol formation pathways during the SOAS campaign. *Atmospheric Chemistry and Physics* **2016**, *16* (22), 14409−14420.

(8) Mentel, T. F.; Springer, M.; Ehn, M.; Kleist, E.; Pullinen, I.; Kurtén, T.; Rissanen, M.; Wahner, A.; Wildt, J. Formation of highly oxidized multifunctional compounds: autoxidation of peroxy radicals formed in the ozonolysis of alkenes−deduced from structure−product relationships. *Atmospheric Chemistry and Physics* **2015**, *15* (12), 6745−6765.

(9) Docherty, K. S.; Wu, W.; Lim, Y. B.; Ziemann, P. J. Contributions of Organic Peroxides to Secondary Aerosol Formed from Reactions of Monoterpenes with O3. *Environmental Science Technology* **2005**, *39* (11), 4049−4059.
(10) Bianchi, F.; Kurtén, T.; Riva, M.; Mohr, C.; Rissanen, M. P.; Roldin, P.; Berndt, T.; Crounse, J. D.; Wennberg, P. O.; Mentel, T. F.; et al. Highly Oxygenated Organic Molecules (HOM) from Gas-Phase Autoxidation Involving Peroxy Radicals: A Key Contributor to Atmospheric Aerosol. *Chem. Rev.* **2019**, *119* (6), 3472−3509.
(11) Pospisilova, V.; Lopez-Hilfiker, F. D.; Bell, D. M.; El Haddad, I.; Mohr, C.; Huang, W.; Heikkinen, L.; Xiao, M.; Dommen, J.; Prévôt, A. S. H.; et al. On the fate of oxygenated organic molecules in atmospheric aerosol particles. *Science Advances* **2020**, *6* (11), No. eaax8922.
(12) Kenseth, C. M.; Hafeman, N. J.; Rezgui, S. P.; Chen, J.; Huang, Y.; Dalleska, N. F.; Kjaergaard, H. G.; Stoltz, B. M.; Seinfeld, J. H.; Wennberg, P. O. Particle-phase accretion forms dimer esters in pinene secondary organic aerosol. *Science* **2023**, *382* (6672), 787−792.
(13) Saliba, G.; Bell, D. M.; Suski, K. J.; Fast, J. D.; Imre, D.; Kulkarni, G.; Mei, F.; Mülmenstädt, J. H.; Pekour, M.; Shilling, J. E.; et al. Aircraft measurements of single particle size and composition reveal aerosol size and mixing state dictate their activation into cloud droplets. *Environmental Science: Atmospheres* **2023**, *3* (9), 1352−1364.
(14) Fast, J. D.; Varble, A. C.; Mei, F.; Pekour, M.; Tomlinson, J.; Zelenyuk, A.; Sedlacek, A. J., Iii; Zawadowicz, M.; Emmons, L. Large spatiotemporal variability in aerosol properties over central Argentina during the CACTI field campaign. *Atmos. Chem. Phys.* **2024**, *24* (23), 13477−13502.
(15) Virkkula, A.; Van Dingenen, R.; Raes, F.; Hjorth, J. Hygroscopic properties of aerosol formed by oxidation of limonene, α-pinene, and β-pinene. *Journal of Geophysical Research: Atmospheres* **1999**, *104* (D3), 3569−3579.
(16) Surratt, J. D.; Kroll, J. H.; Kleindienst, T. E.; Edney, E. O.; Claeys, M.; Sorooshian, A.; Ng, N. L.; Offenberg, J. H.; Lewandowski, M.; Jaoui, M.; et al. Evidence for organosulfates in secondary organic aerosol. *Environ. Sci. Technol.* **2007**, *41* (2), 517−527.
(17) Surratt, J. D.; Gómez-González, Y.; Chan, A. W. H.; Vermeylen, R.; Shahgholi, M.; Kleindienst, T. E.; Edney, E. O.; Offenberg, J. H.; Lewandowski, M.; Jaoui, M.; et al. Organosulfate formation in biogenic secondary organic aerosol. *J. Phys. Chem. A* **2008**, *112* (36), 8345−8378.
(18) Hansen, A. M. K.; Hong, J.; Raatikainen, T.; Kristensen, K.; Ylisirniö, A.; Virtanen, A.; Petäjä, T.; Glasius, M.; Prisle, N. L. Hygroscopic properties and cloud condensation nuclei activation of limonene-derived organosulfates and their mixtures with ammonium sulfate. *Atmospheric Chemistry and Physics* **2015**, *15* (24), 14071−14089.
(19) Tilgner, A.; Schaefer, T.; Alexander, B.; Barth, M.; Collett, J. L., Jr.; Fahey, K. M.; Nenes, A.; Pye, H. O. T.; Herrmann, H.; McNeill, V. F. Acidity and the multiphase chemistry of atmospheric aqueous particles and clouds. *Atmospheric Chemistry and Physics* **2021**, *21* (17), 13483−13536.
(20) Pye, H. O. T.; Nenes, A.; Alexander, B.; Ault, A. P.; Barth, M. C.; Clegg, S. L.; Collett, J. L., Jr.; Fahey, K. M.; Hennigan, C. J.; Herrmann, H.; et al. The acidity of atmospheric particles and clouds. *Atmospheric Chemistry and Physics* **2020**, *20* (8), 4809−4888.
(21) Bertrand, A.; Stefenelli, G.; Pieber, S. M.; Bruns, E. A.; Temime-Roussel, B.; Slowik, J. G.; Wortham, H.; Prévôt, A. S. H.; El Haddad, I.; Marchand, N. Influence of the vapor wall loss on the degradation rate constants in chamber experiments of levoglucosan and other biomass burning markers. *Atmospheric Chemistry and Physics* **2018**, *18* (15), 10915−10930.
(22) Zhang, X.; Cappa, C. D.; Jathar, S. H.; McVay, R. C.; Ensberg, J. J.; Kleeman, M. J.; Seinfeld, J. H. Influence of vapor wall loss in laboratory chambers on yields of secondary organic aerosol. *Proc. Natl. Acad. Sci. U. S. A.* **2014**, *111* (16), 5802−5807.
(23) Surdu, M.; Lamkaddam, H.; Wang, D. S.; Bell, D. M.; Xiao, M.; Lee, C. P.; Li, D.; Caudillo, L.; Marie, G.; Scholz, W.; et al. Molecular Understanding of the Enhancement in Organic Aerosol Mass at High Relative Humidity. *Environ. Sci. Technol.* **2023**, *57* (6), 2297−2309.
(24) Porter, W. C.; Jimenez, J. L.; Barsanti, K. C. Quantifying Atmospheric Parameter Ranges for Ambient Secondary Organic Aerosol Formation. *ACS Earth and Space Chemistry* **2021**, *5* (9), 2380−2397.
(25) Qin, Y.; Ye, J.; Ohno, P.; Zhai, J.; Han, Y.; Liu, P.; Wang, J.; Zaveri, R. A.; Martin, S. T. Humidity Dependence of the Condensational Growth of α-Pinene Secondary Organic Aerosol Particles. *Environ. Sci. Technol.* **2021**, *55* (21), 14360−14369.
(26) Zhang, X.; Lambe, A. T.; Upshur, M. A.; Brooks, W. A.; Gray Bé, A.; Thomson, R. J.; Geiger, F. M.; Surratt, J. D.; Zhang, Z.; Gold, A.; et al. Highly Oxygenated Multifunctional Compounds in α-Pinene Secondary Organic Aerosol. *Environ. Sci. Technol.* **2017**, *51* (11), 5932−5940.
(27) Zhang, X.; McVay, R. C.; Huang, D. D.; Dalleska, N. F.; Aumont, B.; Flagan, R. C.; Seinfeld, J. H. Formation and evolution of molecular products in α-pinene secondary organic aerosol. *Proc. Natl. Acad. Sci. U. S. A.* **2015**, *112* (46), 14168−14173.
(28) Luo, H.; Guo, Y.; Shen, H.; Huang, D. D.; Zhang, Y.; Zhao, D. Effect of relative humidity on the molecular composition of secondary organic aerosols from α-pinene ozonolysis. *Environmental Science: Atmospheres* **2024**, *4* (5), 519−530.
(29) Lopez-Hilfiker, F. D.; Pospisilova, V.; Huang, W.; Kalberer, M.; Mohr, C.; Stefenelli, G.; Thornton, J. A.; Baltensperger, U.; Prévôt, A. S. H.; Slowik, J. G. An extractive electrospray ionization time-of-flight mass spectrometer (EESI-TOF) for online measurement of atmospheric aerosol particles. *Atmospheric Measurement Techniques* **2019**, *12* (9), 4867−4886.
(30) Wang, D. S.; Lee, C. P.; Krechmer, J. E.; Majluf, F.; Tong, Y.; Canagaratna, M. R.; Schmale, J.; Prévôt, A. S. H.; Baltensperger, U.; Dommen, J.; et al. Constraining the response factors of an extractive electrospray ionization mass spectrometer for near-molecular aerosol speciation. *Atmospheric Measurement Techniques* **2021**, *14* (11), 6955−6972.
(31) Platt, S. M.; El Haddad, I.; Zardini, A. A.; Clairotte, M.; Astorga, C.; Wolf, R.; Slowik, J. G.; Temime-Roussel, B.; Marchand, N.; Ježek, I.; et al. Secondary organic aerosol formation from gasoline vehicle emissions in a new mobile environmental reaction chamber. *Atmospheric Chemistry and Physics* **2013**, *13* (18), 9141−9158.
(32) Pospisilova, V.; Bell, D. M.; Lamkaddam, H.; Bertrand, A.; Wang, L.; Bhattu, D.; Zhou, X.; Dommen, J.; Prevot, A. S. H.; Baltensperger, U.; et al. Photodegradation of α-Pinene Secondary Organic Aerosol Dominated by Moderately Oxidized Molecules. *Environ. Sci. Technol.* **2021**, *55* (10), 6936−6943.
(33) Garner, N. M.; Top, J.; Mahrt, F.; El Haddad, I.; Ammann, M.; Bell, D. M. Iron-containing seed particles enhance α-pinene secondary organic aerosol mass concentration and dimer formation. *Environ. Sci. Technol.* **2024**, *58*, 16984−16993.
(34) Bell, D. M.; Imre, D.; Martin, S. T.; Zelenyuk, A. The properties and behavior of α-pinene secondary organic aerosol particles exposed to ammonia under dry conditions. *Phys. Chem. Chem. Phys.* **2017**, *19* (9), 6497−6507.
(35) Bell, D. M.; Pospisilova, V.; Lopez-Hilfiker, F.; Bertrand, A.; Xiao, M.; Zhou, X.; Huang, W.; Wang, D. S.; Lee, C. P.; Dommen, J.; et al. Effect of OH scavengers on the chemical composition of α-pinene secondary organic aerosol. *Environmental Science: Atmospheres* **2023**, *3* (1), 115−123.
(36) Wolfe, G. M.; Marvin, M. R.; Roberts, S. J.; Travis, K. R.; Liao, J. The Framework for 0-D Atmospheric Modeling (F0AM) v3.1. *Geoscientific Model Development* **2016**, *9* (9), 3309−3319.
(37) Jenkin, M. E.; Saunders, S. M.; Pilling, M. J. The tropospheric degradation of volatile organic compounds: a protocol for mechanism development. *Atmos. Environ.* **1997**, *31* (1), 81−104.
(38) Saunders, S. M.; Jenkin, M. E.; Derwent, R. G.; Pilling, M. J. Protocol for the development of the Master Chemical Mechanism, MCM v3 (Part A): tropospheric degradation of non-aromatic volatile organic compounds. *Atmospheric Chemistry and Physics* **2003**, *3* (1), 161−180.

https://doi.org/10.1021/acsestair.5c00064
ACS EST Air 2025, 2, 1565−1574

(39) Bell, D. M.; Zhang, J.; Top, J.; Bogler, S.; Surdu, M.; Slowik, J. G.; Prevot, A. S. H.; El Haddad, I. Sensitivity Constraints of Extractive Electrospray for a Model System and Secondary Organic Aerosol. *Anal. Chem.* **2023**, *95* (37), 13788−13795.
(40) Zhao, J.; Mickwitz, V.; Zhang, J.; Alton, M.; Canagaratna, M.; Graeffe, F.; Schobesberger, S.; Worsnop, D.; Ehn, M. Comparison of Gaseous and Particulate Highly Oxygenated Organic Molecules from the Ozonolysis of Terpenes. *ACS ES&T Air* **2024**, *1* (10), 1294−1303.
(41) Wilson, J.; Imre, D.; Beránek, J.; Shrivastava, M.; Zelenyuk, A. Evaporation Kinetics of Laboratory-Generated Secondary Organic Aerosols at Elevated Relative Humidity. *Environ. Sci. Technol.* **2015**, *49* (1), 243−249.
(42) Baboomian, V. J.; Crescenzo, G. V.; Huang, Y.; Mahrt, F.; Shiraiwa, M.; Bertram, A. K.; Nizkorodov, S. A. Sunlight can convert atmospheric aerosols into a glassy solid state and modify their environmental impacts. *Proc. Natl. Acad. Sci. U. S. A.* **2022**, *119* (43), No. e2208121119.

https://doi.org/10.1021/acsestair.5c00064
ACS EST Air 2025, 2, 1565−1574